SINTER-HARDENING P/M STEELS

Howard G. Rutz, Amie H. Graham, Alan B. Davala

Hoeganaes Corporation, Riverton, NJ 08077

Presented at PM^{2}TEC '97
International Conference on Powder Metallurgy & Particulate Materials
June 29 - July 2, 1997 Chicago, IL USA

ABSTRACT

The use of P/M structural parts is growing in part due to the use of the sinter-hardening process which utilizes high performance materials in combination with an accelerated post sintering cooling rate. The sinter-hardening process offers improved mechanical properties over conventional sintering without a separate heat treatment operation. Thus, where the part design permits, sinter-hardening offers considerable economic benefits to the part producer.

Sinter-hardening typically requires that the P/M steel substantially transform to martensite during cooling. A variety of microstructures and properties can be obtained by varying the post sintering cooling rate. By controlling this rate, the microstructure can be manipulated to produce the required amount of martensite to obtain the desired mechanical properties.

Alloying elements such as molybdenum, nickel, and copper promote hardenability in P/M parts. By increasing the hardenability of the material, the parts can be cooled at slower rates and still produce large amounts of martensite. The ability to increase the amount of martensite, leading to increased strength and hardness,

through the use of proper alloy selection and accelerated cooling rate will be discussed.

INTRODUCTION

Sinter-hardening refers to a process where the cooling rate experienced in the cooling zone of the sintering furnace is fast enough that a significant portion of the material matrix transforms to martensite. Interest in sinter-hardening has grown because it offers good manufacturing economy by providing a one step process and a unique combination of strength, toughness, and hardness [1].

A variety of microstructures and properties can be obtained by

varying both the alloy type and content as well as the post sintering cooling rate. By controlling the cooling rate, the microstructure can be manipulated to produce the required proportion of martensite which will lead to desired mechanical properties [1-3]. By understanding how the sintering conditions affect the microstructure, materials can be modeled to produce the final properties that are desired.

A graphical way of examining the effects of alloying elements on the final microstructure of a steel is by using the characteristic isothermal transformation (I -T) diagram. This indicates the time necessary for the for the isothermal transformation to start and finish as well as the cooling time and temperature combinations needed to produce the final microstructure.

As the composition of a steel is changed, the effects are seen in the l-T diagram for that material. Figures 1a and 1b compare two materials that are similar in composition except for a 0.24 w/o molybdenum addition in Figure 1b [4]. An apparent shift in the nose of curve to the right is seen in the material with the molybdenum addition. This indicates that the maximum allowable time to reach the nose of the curve is longer. Due to this shift, martensite can be produced at slower cooling rates, hence the material has a higher hardenability. Similar effects can be demonstrated for other alloying elements such as nickel, copper, manganese and chromium.

Figures 2a and 2b compare two materials with similar compositions except for carbon content [5]. Figure 2a depicts a material with 0.47 w/o carbon while Figure 2b depicts a material with 0.68 w/o carbon. There is a small shift in the curve to the right with the addition of carbon. This indicates that the addition of carbon has only a small effect on the hardenability of a material.

In most cases, a steel is not isothermally transformed at a temperature above the martensite start temperature but is continuously cooled from the austenite temperature to room temperature. The transformation from austenite to pearlite occurs over a range of temperatures rather than at a single isothermal temperature. The final microstructure after continuous-cooling may be complex.

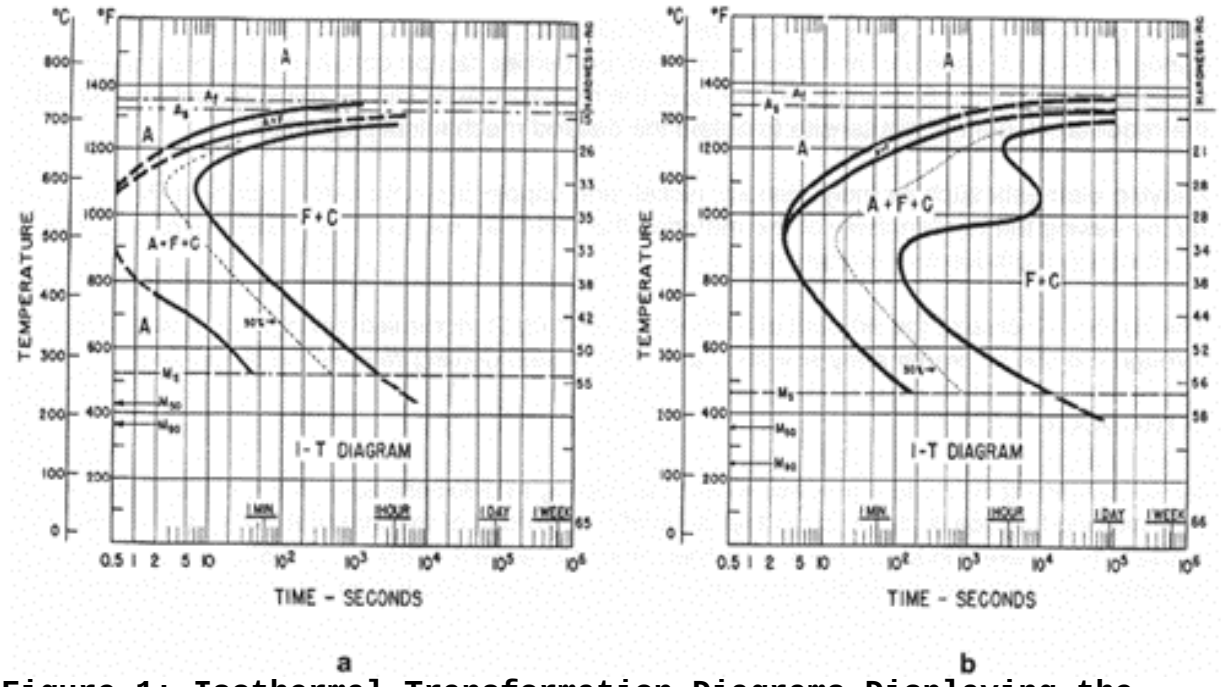

Figure 1: Isothermal Transformation Diagrams Displaying the Effect of Molybdenum Additions

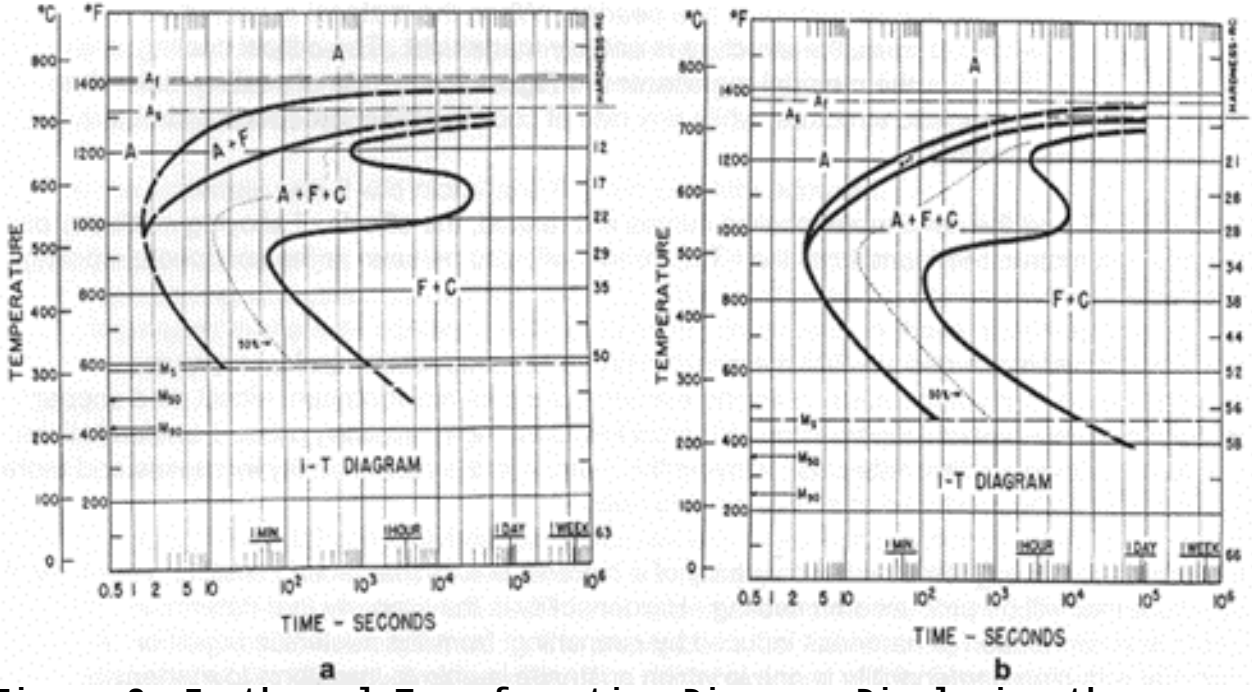

Figure 2: Isothermal Transformation Diagrams Displaying the Effect of Carbon

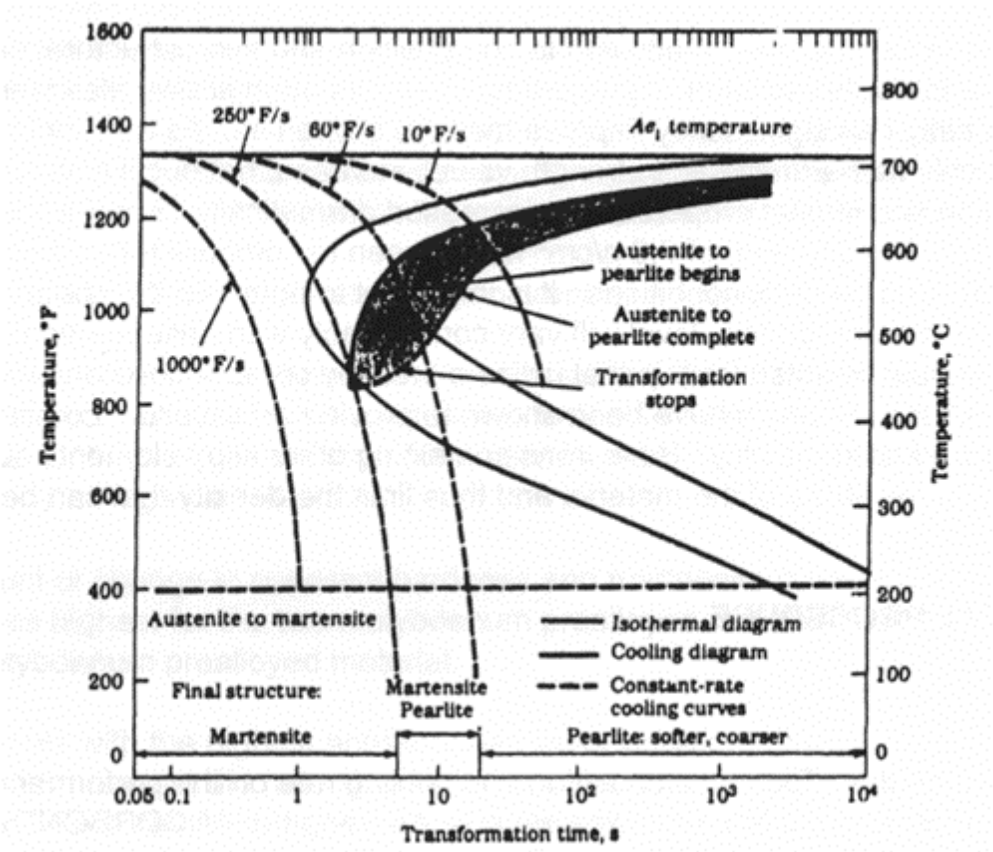

Figure 3: Continuous-Cooling Diagram Displaying the Variation in Microstructure as a Function of Cooling Rate

Figure 3 shows a continuous-cooling diagram superimposed over an l-T diagram for a steel [6].

In the continuous-cooling diagram, the transformation start and finish are shifted to longer times and slightly lower temperatures as compared with the l-T diagram. When this steel is slow cooled (l0°F/s), the microstructure is coarse pearlite. When the cooling rate of the material is increased (60°F/s), the microstructure is fine pearlite. When the material is cooled so rapidly that no pearlite is able to form, the structure is entirely martensite. The critical cooling rate in this case is 250°F/s. For the material represented in Figure 3, any rate of cooling faster than this produces a martensitic structure, while any rate of cooling slower produces a structure containing some pearlite.

Since the l-T and the continuous-cooling curves are related, the effects of alloying additions on the final microstructure found from the l-T diagrams will also be seen in the continuous-cooling diagrams.

Alloying elements are used in P/M materials to promote hardenability and increase the mechanical strength of the parts. Alloying elements such as molybdenum, nickel, and copper move the continuous cooling transformation curves to the right, allowing phase transformations to occur at slower cooling rates. By alloying the materials, the hardenability increases and more martensite can be produced at similar cooling rates.

In addition to cooling rate, the hardenability of a material is a critical factor in defining the type of structure that will be produced on cooling. Hardenability is the property that determines the depth and distribution of hardness induced by quenching from the austenitic condition. A material with high hardenability is one in which austenite is able to transform to martensite without forming pearlite, even when the rate of cooling is rather slow. Optimal sinter-hardening materials would have a high hardenability, so that the cooling rates needed to produce large proportions of martensite will be attainable.

It is important to remember that in addition to composition and microstructure, density plays an important role in the determination of properties. [7] It has been shown elsewhere that increases in density can significantly improve material properties. As density levels are increased, not only do hardness and strength values increase, but ductility values such as tensile elongation and impact properties are increased dramatically. For the tests described below, a moderate density level of 7.0 g/cm^3 was chosen to compare the properties of the various materials and process conditions. It is important to note that the compaction pressure required to reach a given density level will vary considerably with base material selected. Two of the base materials selected for this trial utilize a prealloy composition containing only molybdenum. These materials have been shown to provide an excellent combination of compressibility and hardenability. Base irons containing other alloy elements such as nickel, can limit the compressibility of the material and thus limit the density that can be achieved.

EXPERIMENTAL PROCEDURE

Materials

In order to evaluate the effect of composition and cooling rate on the performance of several materials, seven 500-pound test premixes were made using the ANCORBOND® process. The premixes were chosen to study the effects of molybdenum and nickel as prealloyed additions, and nickel, copper, and graphite as premix additions. The premix compositions are shown in Table I. In all cases 0.75 w/o Lonza Acrawax was added to the mixes. The nickel

utilized in the premixes was Inco 123, the copper was ACuMet -200 mesh atomized copper powder, and the graphite was Asbury 3203 SCR HS.

Test Specimen Preparation

All samples were prepared and tested according to the appropriate MPIF standard [8]. Specimens nominally 0.45 inches x 0.45 inches x 3.5 inches (11.4 mm x 11.4 mm x 88.9 mm) were compacted to a green density of 7.0 g/cm^3. Once sintered, the specimens were tempered at 380°F (193°C) in air for 1.5 hours and machined into threaded tensile test pieces.

Table I: Premix Compositions

		Prealoyed Additions		Premix Additions		
Mix	**Base**	**Ni (w/o)**	**Mo (w/o)**	**Cu (w/o)**	**Ni (w/o)**	**Graphite (w/o)**
1	Ancorsteel ® 85 HP	--	0.85	--	2.00	0.50
2	Ancorsteel 150 HP	--	1.50	--	2.00	0.50
3	Ancorsteel 85 HP	--	0.85	1.00	2.00	0.50
4	Ancorsteel 150 HP	--	1.50	1.00	2.00	0.50
5	Ancorsteel 85 HP	--	0.85	2.00	--	0.90
6	Ancorsteel 150 HP	--	1.50	2.00	--	0.90
7	Ancorsteel 4600 V	1.85	0.55	2.00	--	0.90

Sintering

All test pieces were sintered under production conditions at Clarion Sintered Metals. The Abbott furnace used in the study was equipped with a VARICOOL post sintering cooling system which combines radiant and convection cooling to accelerate the cooling capabilities of the continuous belt furnace. The VARICOOL system is easily adjustable which facilitates controlling the atmosphere re-circulation to optimize the cooling profile.

Two sintering cycles were examined in order to evaluate the effect of cooling rate on the properties of the selected materials as follows:

Cycle One
Sintering Temperature: 2050°F (1120°C)
Atmosphere: 7 v/o H_2, 93 v/o N_2

Belt Speed:	4.8 in/mm
VARICOOL Setting:	100%

Cycle Two	
Sintering Temperature:	2050°F (1120°C)
Atmosphere:	7 v/o H_2, 93 v/o N_2
Belt Speed:	4.8 in/mm
VARICOOL Setting:	50%

At these settings the parts were at sintering temperature for about 30 minutes. The sintered parts were stress relieved at 380°F (193°C) in air for 1.5 hours prior to machining.

Testing

Following tempering, apparent hardness measurements were performed on the surface of the specimens using a Rockwell hardness tester. All of the testing was performed on the Rockwell C scale for comparison purposes. Although some values were below the minimum for this scale, as suggested by ASTM standard E 18 - 94 [9], this single scale was utilized to provide a comparison between a relatively large range of hardness values generated during the tests.

Tensile testing was performed on round threaded tensile test pieces with a gauge length of 1 inch (25.4 mm) and a nominal diameter of 0.20 inches (5.08 mm). Testing was performed on a 60,000 pound Tinius Olsen universal testing machine at a crosshead speed of 0.025 inches/minute. Elongation values were determined utilizing an extensometer with a range of 0 to 20%. The extensometer was left on to failure.

Metallography

The tensile bars were sectioned and prepared for metallographic analysis. Photomicrographs were taken of the structures following a 2% nital/4% picral etch. The martensite content was determined utilizing point count analysis. This analysis technique included the porosity as a portion of the total microstructure. The reported percentages were corrected by eliminating the 11% porosity present in these materials (the approximate porosity amount at a density of 7.0 g/cm^3) so that only the metallic portion of the microstructure is considered.

RESULTS

The apparent hardness, ultimate tensile strength, yield strength, total elongation, and martensite content of the test pieces are represented in Table II. Photomicrographs, taken at original

magnification of 500X, of the different materials are shown in Figures 4-10.

Table II: Properties of the Material Matrix

Mix	VARICOOL Setting (%)	Apparent Hardness (HRC)	0.2% Offset YS (psi x 10^3/MPa)	UTS (psi x 10^3/MPa)	Elg. (%)	Martensite Content (%)
1	50	6	66.5/459	90.5/624	2.4	7.3
1	100	9	70.2/484	97.1/669	2.3	20.8
2	50	12	80.5/555	103.5/714	1.6	10.1
2	100	16	87.0/600	110.3/760	1.5	11.8
3	50	7	71.6/494	98.1/676	2.0	23.0
3	100	11	78.5/541	107.9/744	1.9	38.8
4	50	14	89.7/618	114.3/788	1.9	38.8
4	100	19	98.1/676	122.4/844	1.4	20.2
5	50	21	95.2/656	109.5/755	1.1	22.5
5	100	30	112.6/776	135.9/937	1.2	66.3
6	50	25	102.7/708	132.0/910	1.5	29.8
6	100	35	114.7/791	127.1/876	1.0	60.1
7	50	35	102.4/706	118.9/820	1.1	71.9
7	100	37	106.3/732	117.9/813	0.9	95.5

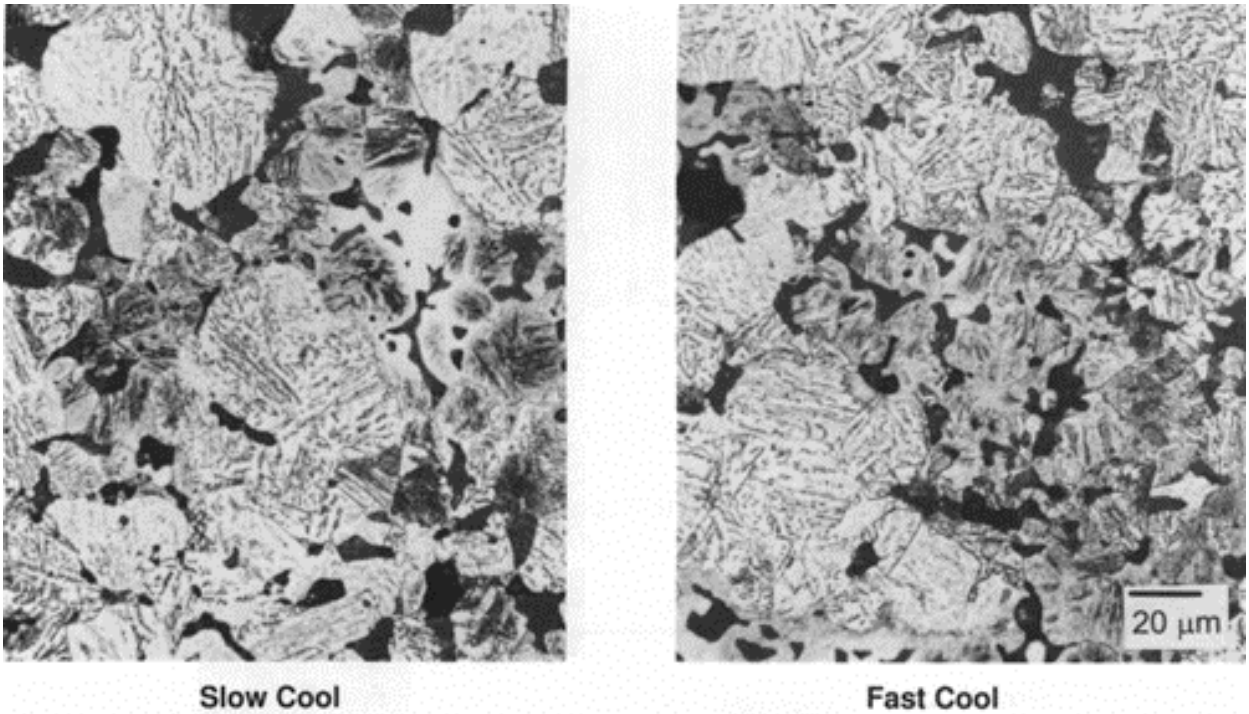

Figure 4: Photomicrographs of Mix 1 (Original Magnification 500X)

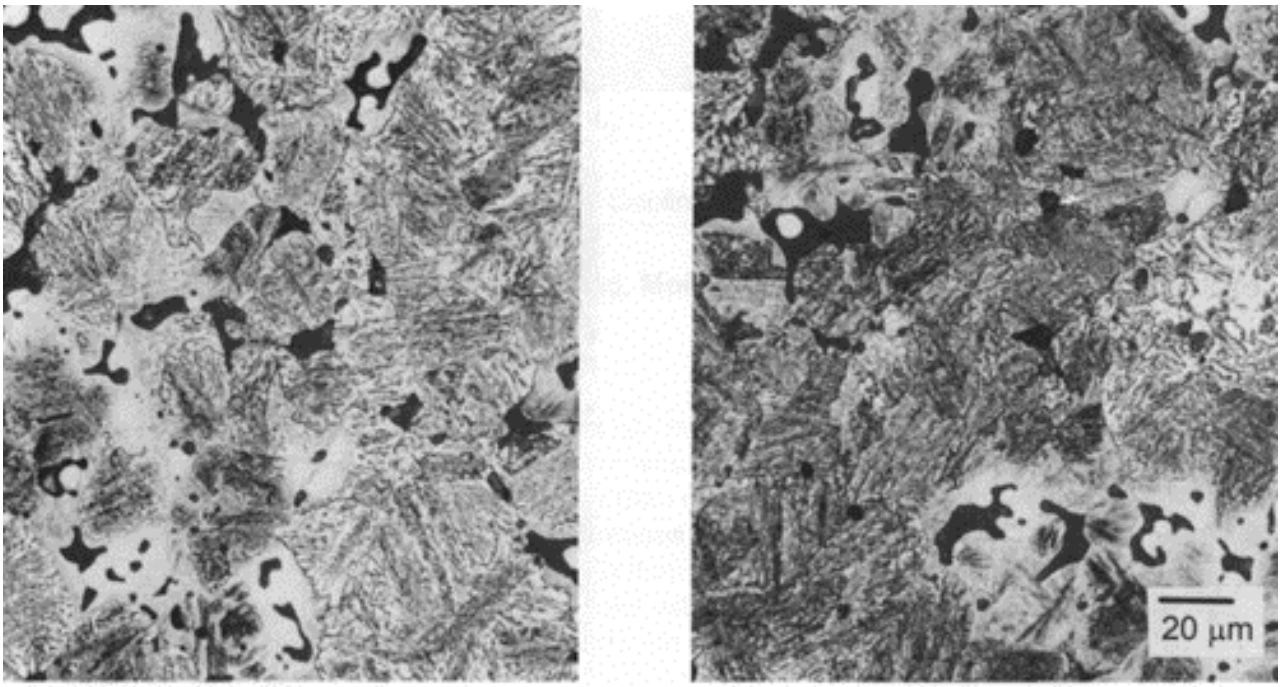

Slow Cool Fast Cool

Figure 5: Photomicrographs of Mix 2 (Original Magnification 500X)

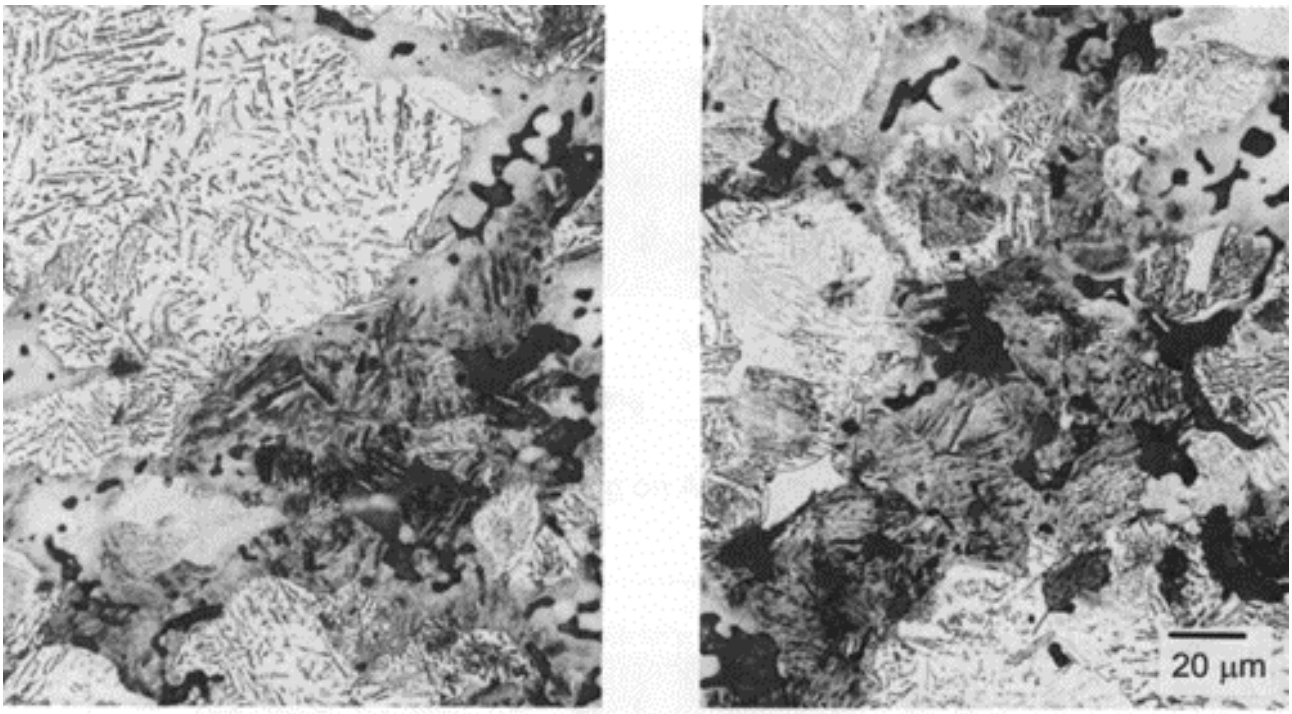

Slow Cool Fast Cool

Figure 6: Photomicrographs of Mix 3 (Original Magnification 500X)

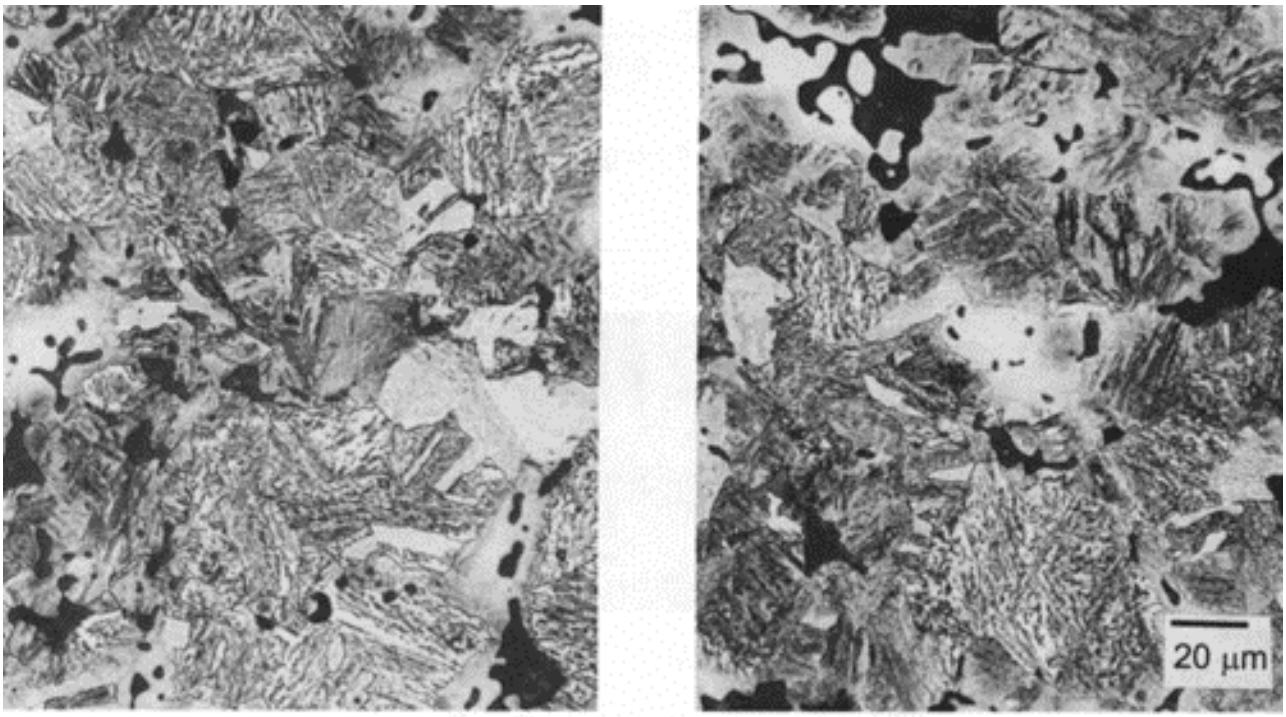

Slow Cool Fast Cool

Figure 7: Photomicrographs of Mix 4 (Original Magnification 500X)

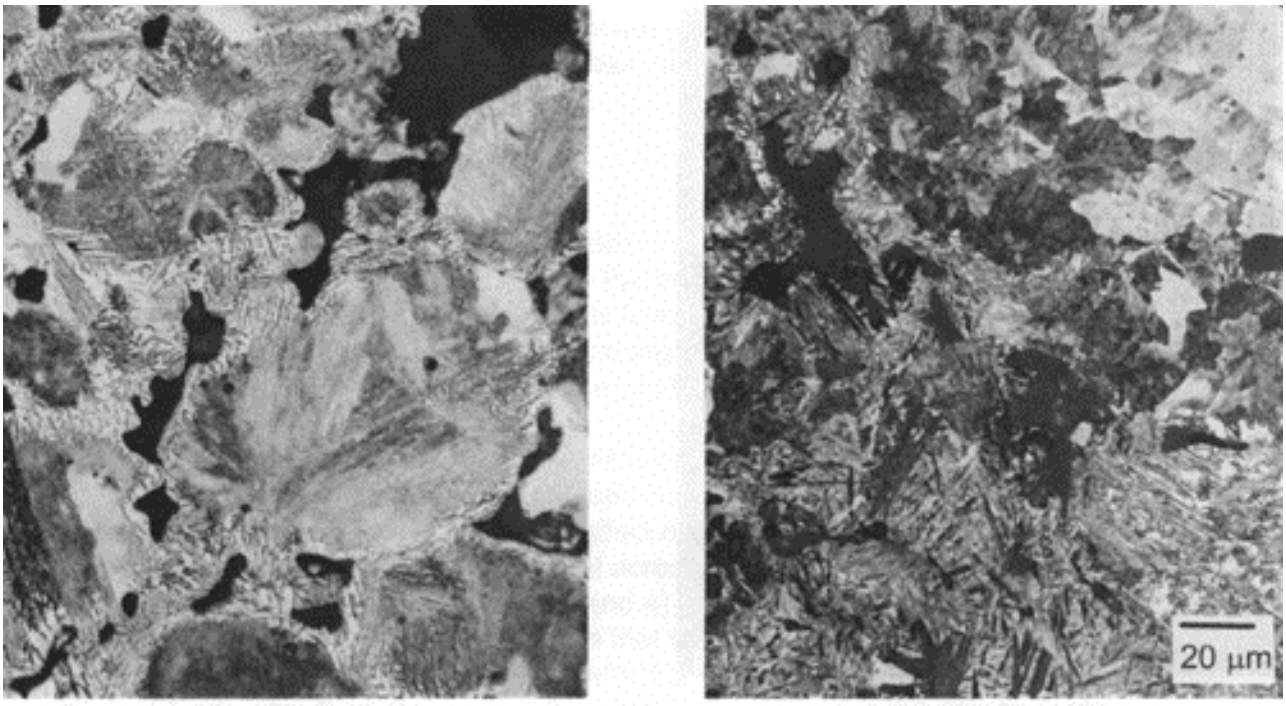

Slow Cool Fast Cool

Figure 8: Photomicrographs of Mix 5 (Original Magnification 500X)

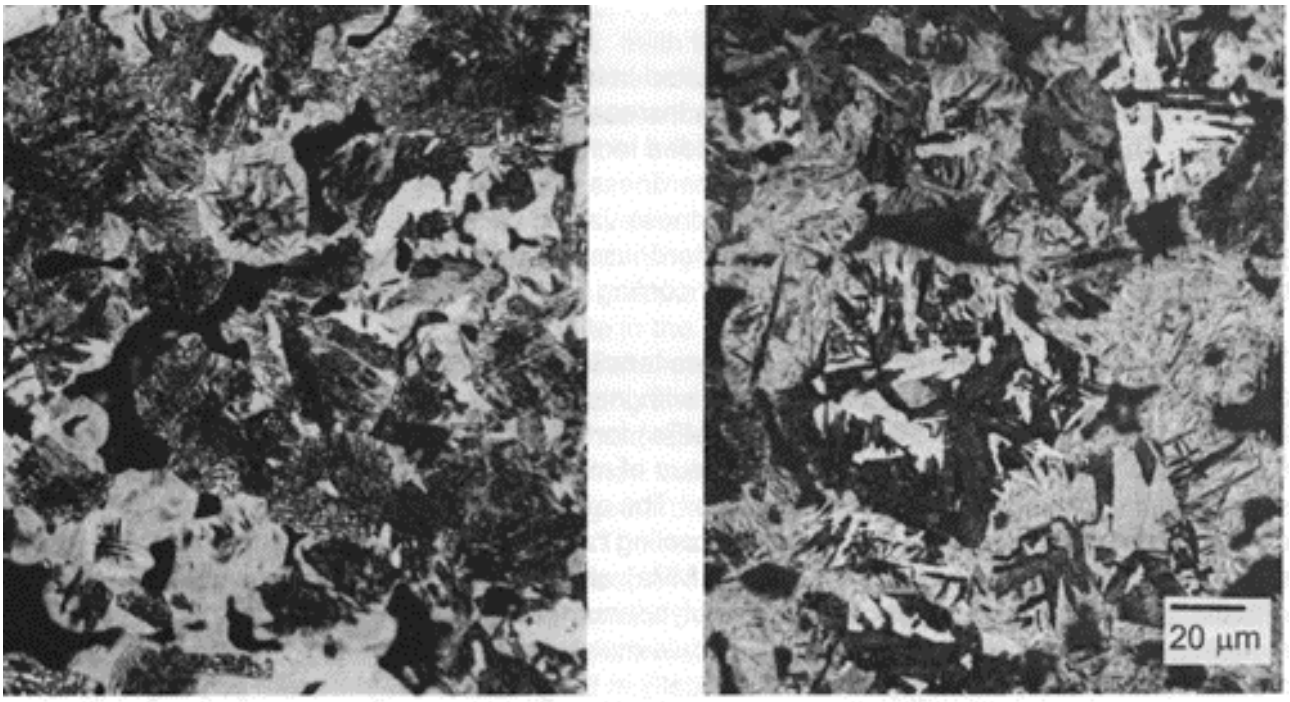

Figure 9: Photomicrographs of Mix 6 (Original Magnification 500X)

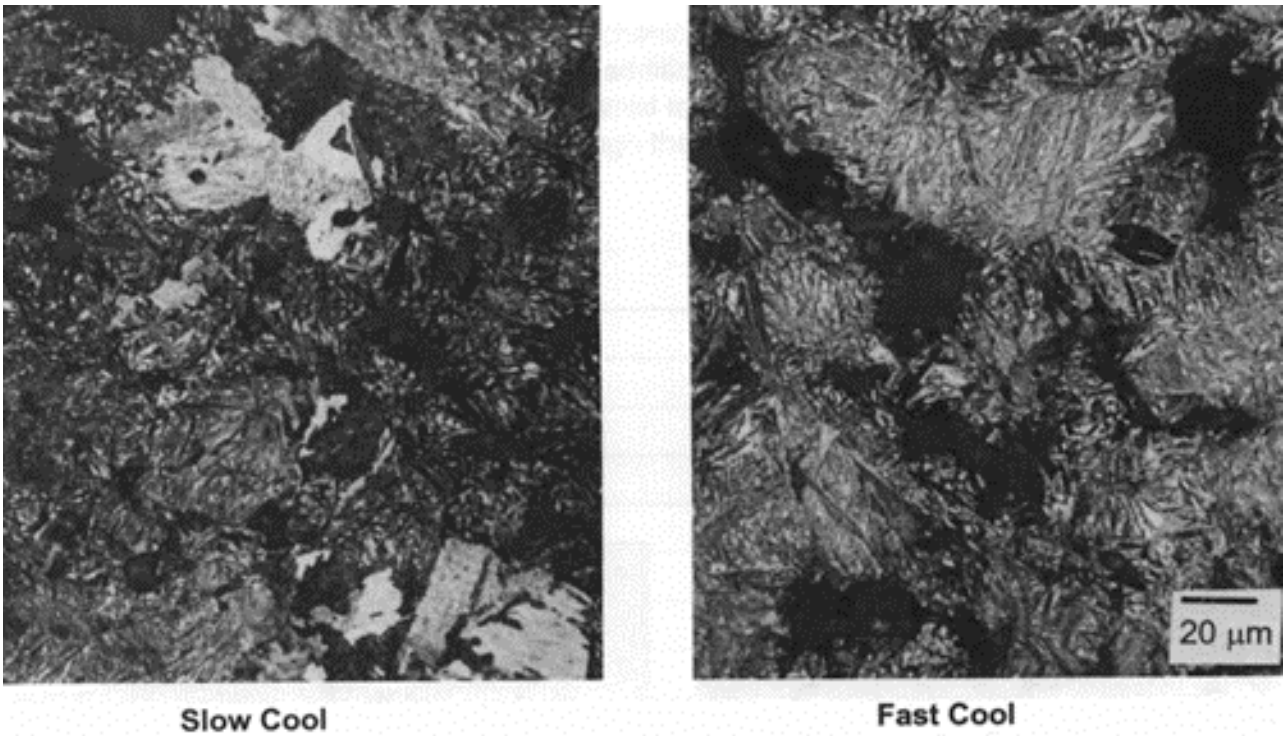

Figure 10: Photomicrographs of Mix 7 (Original Magnification 500X)

DISCUSSION

The Effect of Cooling Rate

As expected, increasing the cooling rate resulted in increased apparent hardness and strength values. On the whole, hardness values were increased between 2 to 10 HRC for a given material. The mixes with 0.5 w/o graphite added increased 3 to 5 HRC, with the amount of change increasing for materials with higher hardness values. The mixes with 0.9 w/o graphite added indicated the largest difference in hardness values with the increases ranging from 2 to 10 HRC. Mix 7 which exhibited the highest hardness values at the higher cooling rate, showed the smallest increase in hardness with faster cooling.

The 0.2% offset yield strength and the ultimate tensile strength values for the mixes with 0.5 w/o graphite all showed increased levels with increasing cooling rate. The yield strength increased from 3,700 to 8,400 psi (26 to 58 MPa) for this group while the UTS increased from 6,600 to 9,800 psi (46 to 68 MPa). In this group of materials, the elongation dropped only slightly as the result of the faster cooling rate. The effects in the mixes with 0.9 w/o graphite additions were quite different. Increases in cooling rates resulted in improvements in yield strength from 3,900 to 17,400 psi (27 to 120 MPa) with the highest effect occurring in the mix with the lowest prealloy content (0.85 w/o molybdenum) and the lowest in the mix with the highest alloy content (1.55 w/o nickel +0.55 w/o molybdenum). This basic trend is continued in the UTS where the UTS in improved dramatically in the 0.85 w/o molybdenum prealloy but actually decreases in the other two, more highly alloyed materials. Again, with the exception perhaps of the 1.5 w/o molybdenum prealloy, no significant decrease in elongation was noted.

As expected, in all materials, the percent of martensite present increased significantly with the increase in cooling rate. The effect of the increased martensite levels is apparent in the hardness values for each of the materials. The effect of the higher levels of martensite on tensile properties is less obvious. In several cases, materials with significantly lower percentages of martensite and lower hardness values demonstrated higher tensile strengths. This will be discussed in some detail below.

The Effect of Alloy Content

The selection of the mix compositions was designed to allow the study of the effect of several different additions. Mixes 1 through 4 allow the evaluation of both molybdenum prealloy levels and copper premix additions at a fixed admix level of 2 w/o

nickel and a moderate level of 0.5 w/o graphite. Mixes 5 through 7 allow the study of the effect of several prealloy chemistries on a fixed admixed chemistry of 2 w/o copper and a higher level of 0.9 w/o graphite.

Figures 11 through 20 compare the hardness, yield strength, UTS and elongation values for Mixes 1 through 4. As noted above, increased cooling rates resulted in improved hardness and strength values for all four materials. The effect of increasing cooling rate on individual materials appears to be relatively consistent across the four mixes. The mixes with the lowest and highest level of alloy content (Mixes 1 and 4) exhibit the lowest and highest values of hardness and strength. The results indicate that the increase in prealloy content from 0.85 w/o to 1.5 w/o molybdenum has a more potent effect on hardness and strength than the admix addition of 1 w/o copper. For example, the additional 0.65 w/o molybdenum results, on average, in an increase of 7 HRC and about 14,000 psi (97 MPa) in UTS. The addition of 1 w/o copper results, on average, in an increase of 2 HRC and approximately 10,000 psi (69 MPa) in UTS. The results are surprisingly consistent across each material pair. The elongation values follow a reverse trend, with the leaner alloyed materials exhibiting higher ductility.

In terms of microstructure (Figures 4 through 7), in all four cases, the faster cooling rate increases the amount of martensite present. With this group of materials, it appears that the increased transformation to martensite with the accelerated cooling occurs predominantly in the nickel rich areas which remain as retained austenite in the slow cooled materials. In all cases the faster cooling rate also appears to result in a finer pearlite structure.

Perhaps most interesting is the relationship between the two materials based on the 0.85 w/o and the 1.5 w/o molybdenum materials. Surprisingly, the lower molybdenum materials generally contain higher levels of martensite than the comparably processed materials made from the 1.5 w/o molybdenum base iron. The pearlite in the 1.5 w/o molybdenum materials appears to be very different than the 0.85 w/o molybdenum materials. The higher molybdenum content appears to result in much finer pearlite spacing and perhaps a higher percentage of carbide present within the pearlite structure. Microhardness evaluations of these structures were carried out with faster cooled versions of Mixes 1 and 2. The pearlite structure in Mix 1 (0.85 w/o molybdenum) indicates an average hardness of 219 HV_{50} while the martensite exhibits an average hardness of 314 HV_{25}. The results for Mix 2 (1.5 w/o molybdenum) indicate nearly identical results for the martensite areas at 327 HV_{25} but the finer pearlite exhibits a hardness of 306 HV_{50}. The exact mechanism for this result is

unclear but might be supported by the presence of less martensite in the 1.5 w/o molybdenum materials. If there is more carbon tied up in the pearlite structure of the higher molybdenum containing material, the nickel rich area may then be carbon poor and not transform. Further studies are warranted to investigate the exact nature of the microstructures. However, despite the lower level of martensite found in the 1.5 w/o molybdenum materials, the hardness and strength is significantly higher than that found in comparably processed 0.85 w/o molybdenum materials.

It is important to note that while these materials indicate excellent results from accelerated cooling, they would not be traditionally thought of as “sinter-hardening” materials. Normally, increases in graphite contents in the 0.7 to 0.9 w/o range would be recommended to maximize hardness values. The results do show how mechanical properties can be modified for a wide variety of materials not only by the presence of additional martensite, but by control of the microstructure as a whole. Further work is required to understand the role of various admix additions in the development of properties through the use of accelerated cooling.

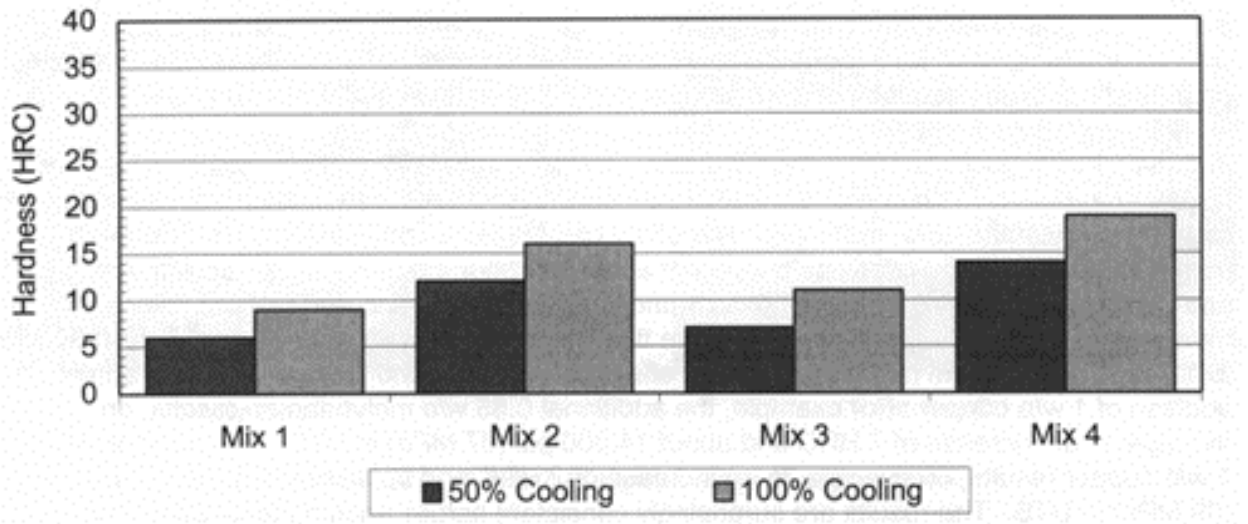

Figure 11: Effect of Accelerated Cooling, Molybdenum Content, and Alloy Additions on Apparent Hardness

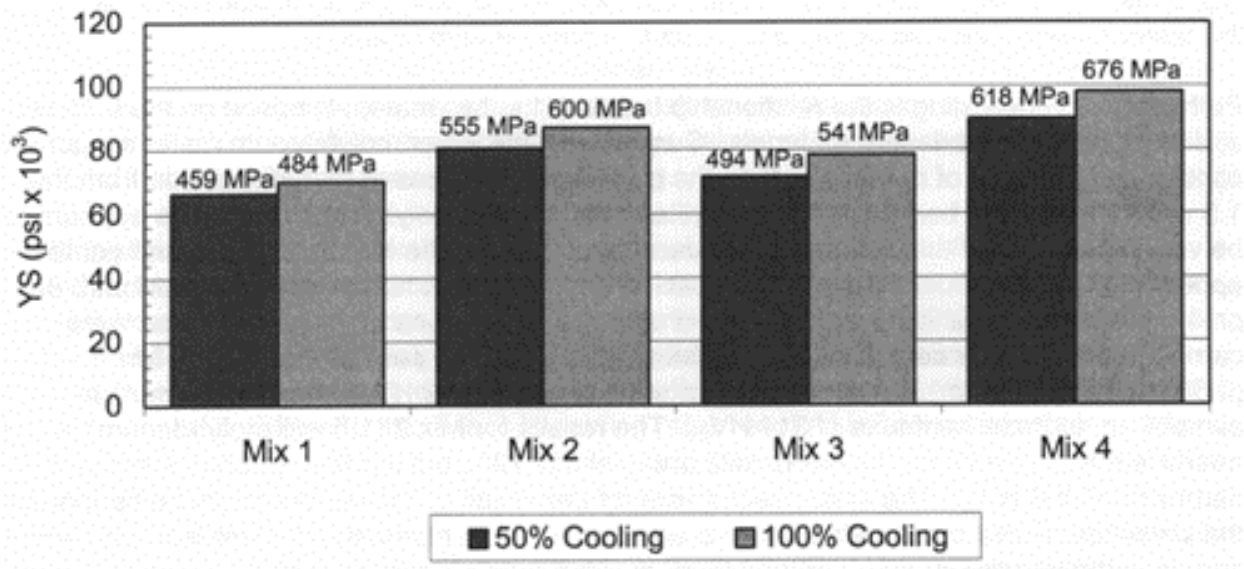

Figure 12: Effect of Accelerated Cooling, Molybdenum Content, and Alloy Additions on 0.2% Offset Yield Strength

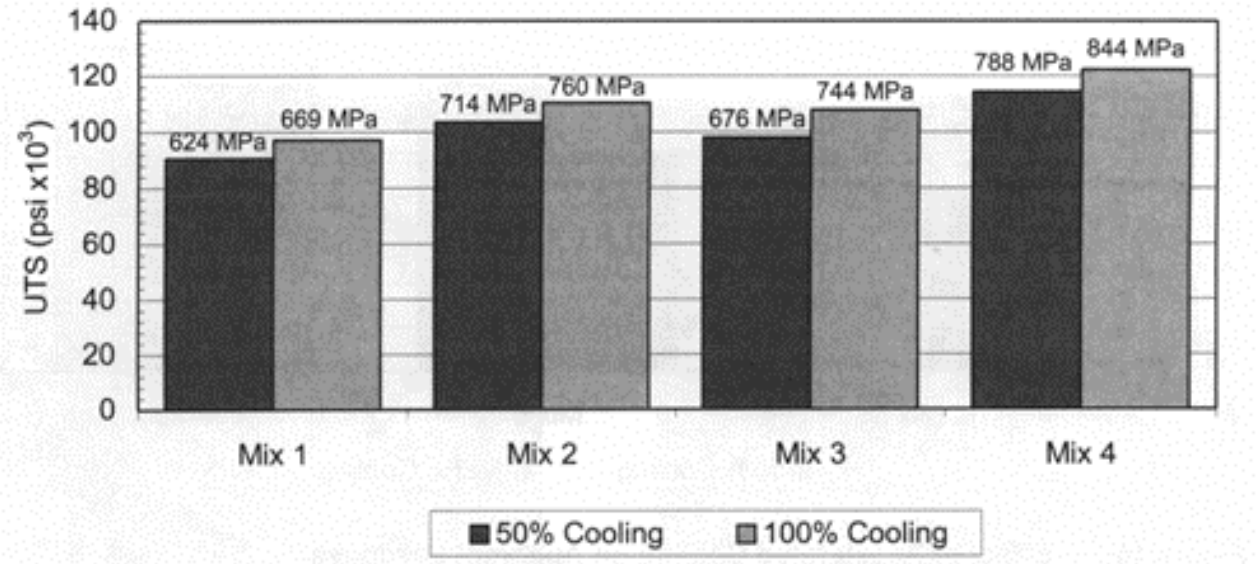

Figure 13: Effect of Accelerated Cooling, Molybdenum Content, and Alloy Additions on Ultimate Tensile Strength

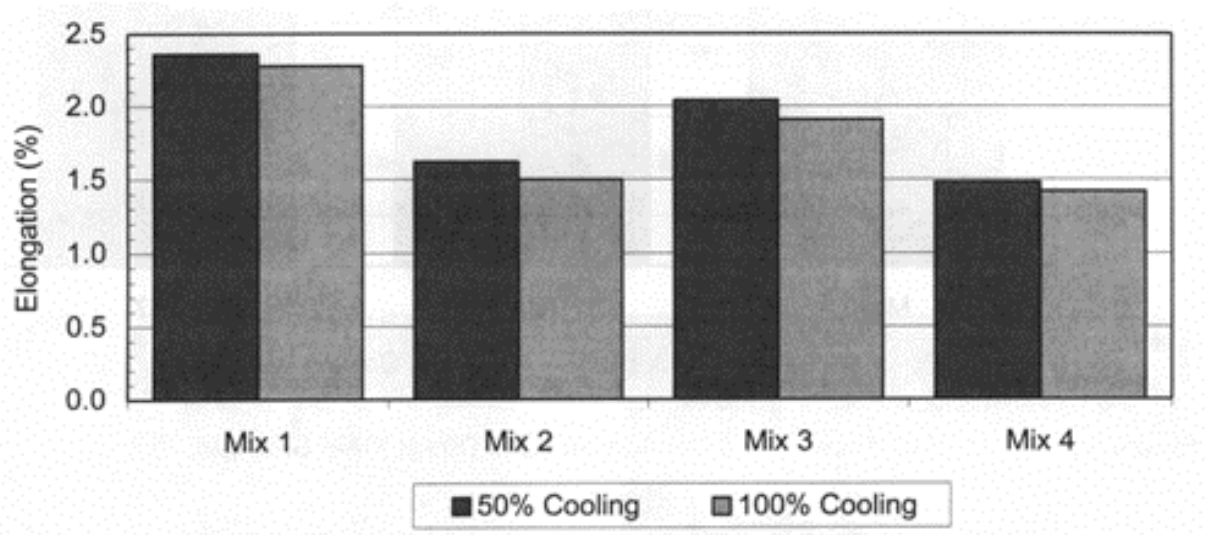

Figure 14: Effect of Accelerated Cooling, Molybdenum Content, and Alloy Additions on Elongation

Figures 15 through 18 compare the apparent hardness, yield strength, UTS and elongation values for Mixes 5 through 7. The effect of increased cooling rate and alloy content appear to be more complex with this series of materials than noted above for those with the lower graphite content. In all three cases, the hardness increases with faster cooling rates but the amount of increase is significantly less for Mix 7 (2 HRC) than for Mixes 5 and 6 (9 and 10 HRC). Mix 5 shows large increases in tensile strength values with increasing cooling rate. Mixes 6 and 7 show less of an increase in yield strength and both actually indicate decreases in UTS with increased cooling rate. Thus, the highest tensile properties are not found in those materials exhibiting the highest hardness values but in the fast cooled version of Mix 5 and the slow cooled version of Mix 6.

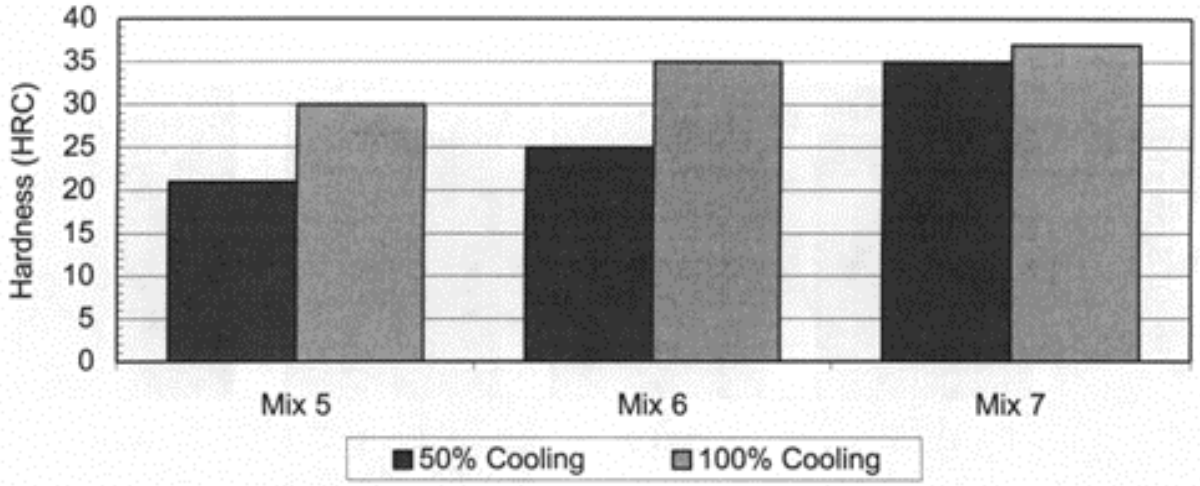

Figure 15: Effect of Accelerated Cooling on Apparent Hardness

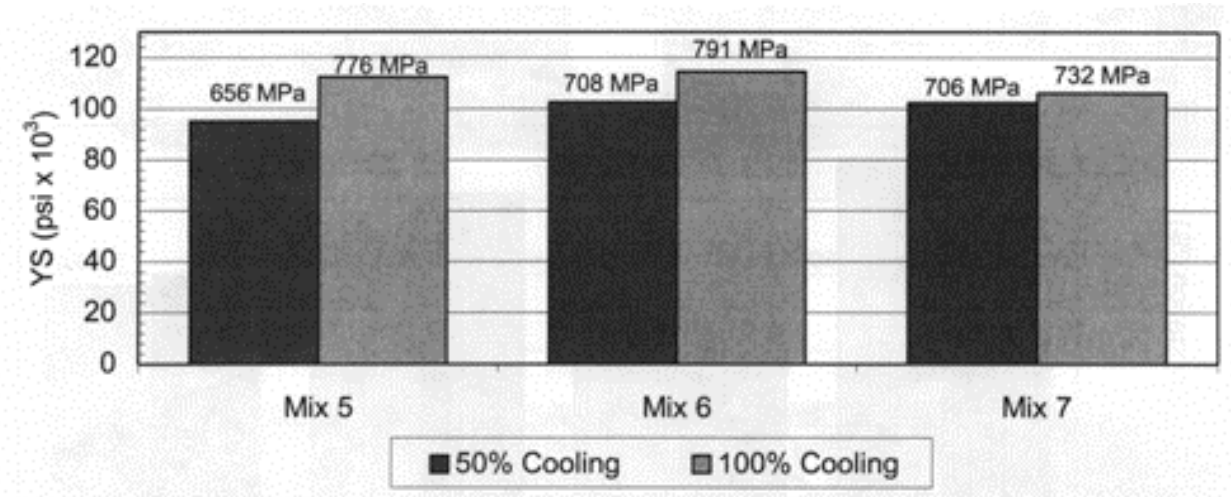

Figure 16: Effect of Accelerated Cooling on 0.2% Offset Yield Strength

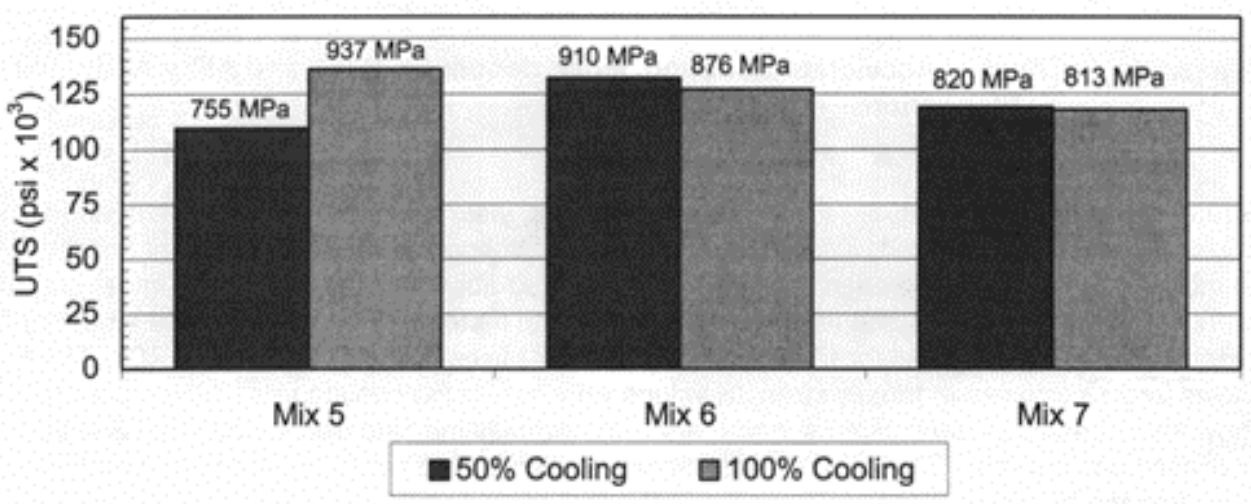

Figure 17: Effect of Accelerated Cooling on Ultimate Tensile Strength

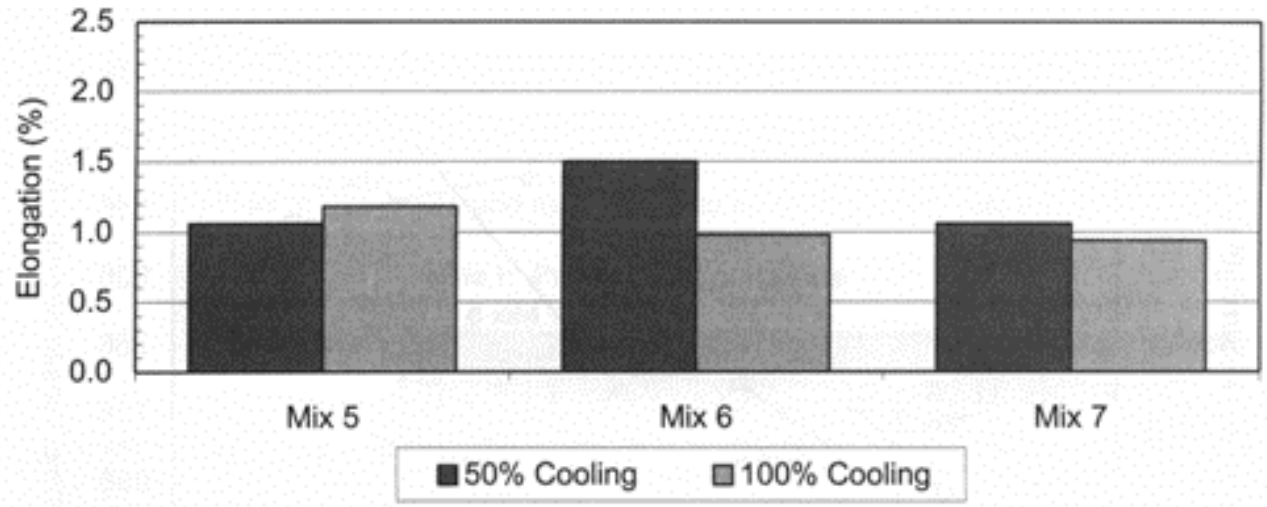

Figure 18: Effect of Accelerated Cooling on Elongation

The microstructures of these materials support the results noted above (Figures 8-10). The amount of martensite present in Mixes 5 and 6 is increased significantly with the higher cooling rate thus resulting in large increases in apparent hardness values. Mix 5 shows the largest change in microstructure, going from predominantly unresolved pearlite with a slow cool to mostly martensite following accelerated cooling. The microstructures correspond well with the large increase in strength determined for this material. Mix 7, on the other hand, contains a significant portion of martensite in the slow cooled state, so the small additional increase in martensite content resulting from faster cooling rates has only a minor effect on hardness. It should also be noted that the fast cooled versions of Mixes 6 and

7 as well as the slow cooled version of Mix 7 appear to contain a significant amount of retained austenite. The exact amount of this phase is difficult to determine optically on these samples.

Figure 19 shows the relationship between apparent hardness values and ultimate tensile strength. There appears to be good correlation between the hardness and strength but the graph highlights several additional points. At the low values of hardness, the strength increases rapidly for a given increase in hardness. The rate of increase in strength appears to peak at hardness levels of between 25 and 30 HRC. For hardness levels above 30 HRC, the strength appears to be decreasing with increasing hardness values for the materials tested. An additional comparison can be made with Mixes 1 through 4. Mixes 1 and 2, containing both high and low levels of molybdenum but only nickel as the admixed ingredient, showed very good correlation between hardness and UTS. Mixes 3 and 4, with the added copper, also show a good correlation but, the addition of copper appears to raise the UTS value for a given level of hardness.

Figure 20 indicates the relationship between the martensite level and the ultimate tensile strength. Mixes 1 through 4 again show a unique correlation. The materials with 0.85 w/o molybdenum (Mixes 1 and 3) indicated good correlation with each other but fairly low ultimate strength for the given level of martensite. The materials with the higher level of molybdenum (Mixes 2 and 4) show a good correlation with each other but much higher strength for a given level of martensite. Overall, the trend follows in a similar fashion to that noted with hardness values. The strength increases with increased levels of martensite until peaking at around 60% martensite, after which further increases in martensite level actually result in lower strength values. Further investigations will be needed to determine if the presence of retained austenite or other factors cause this decrease in strength.

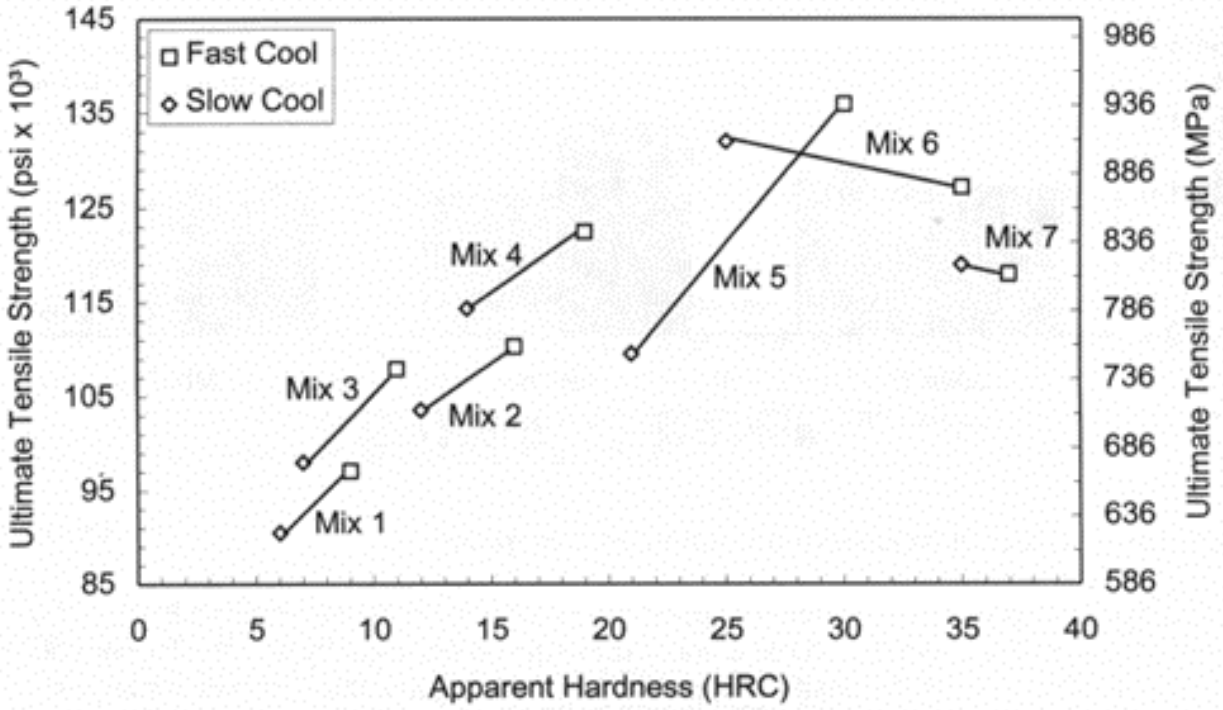

Figure 19: The Relationship between Apparent Hardness and Ultimate Tensile Strength for the Tested Materials

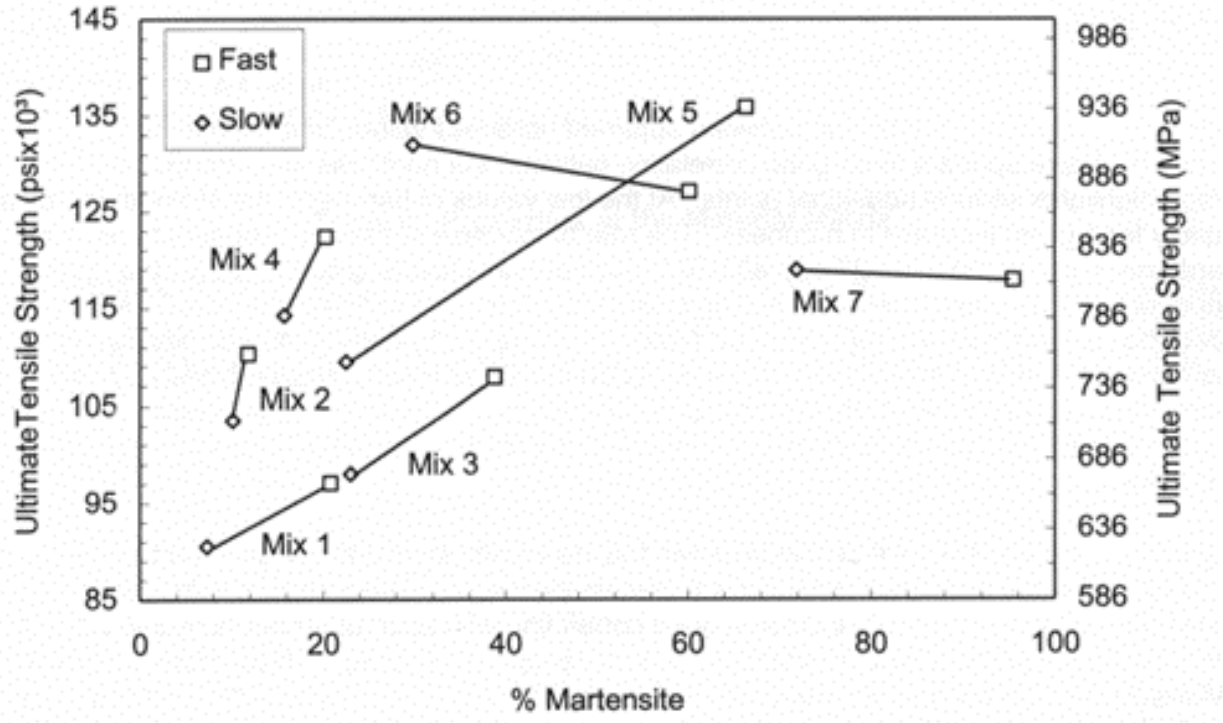

Figure 20: The Relationship between Martensite and Tensile Strength for the Tested Materials

CONCLUSIONS

A study was conducted on two families of materials in order to evaluate the effect of post-sintering cooling rate on microstructure and the resulting mechanical properties. The results may be summarized as follows:

1. For the materials with 2 w/o nickel and 0.5 w/o graphite admixed:

- Accelerated cooling resulted in increased strength and apparent hardness while decreasing elongation values only slightly. This result was the consequence of increased martensite content and finer pearlitic structures. In these materials, the martensite was the result of transformation of nickel rich areas in the microstructure.

- The increase in prealloyed alloy content from 0.85 w/o to 1.5 w/o molybdenum resulted in a larger increase in strength than the addition of 1.0 w/o admixed copper.

- Although the 0.85 w/o molybdenum materials exhibited higher percentages of martensite than identical chemistries based on the 1.5 w/o molybdenum prealloyed material, the higher molybdenum materials had higher apparent hardness and strength values. This surprising result was explained by the presence in the 1.5 w/o molybdenum based material of significantly finer pearlite. The microhardness of this finer pearlite structure approached that of the martensite and thus had a significant influence on the performance.

- It was also noted that these four materials are clearly not optimized to provide high apparent hardness values. It was suggested that additional work is called for with higher graphite contents to obtain high martensite contents and apparent hardness values above 30 HRC. The study did indicate that accelerated cooling has benefit to the P/M parts fabricator beyond simply creating very hard materials. The use of this system may allow leaner alloy materials to attain higher properties while reducing material cost.

2. For the material with 2 w/o copper and 0.9 w/o graphite admixed:

- As the cooling rate was increased for these materials, the apparent hardness increased. This was associated with higher martensite contents in the faster cooled materials. Martensite contents of greater than 50% were found in all three base

materials when accelerated cooling was utilized.

- The amount of change in apparent hardness and martensite content with accelerated cooling was highest for the two molybdenum prealloyed materials and least for the nickel/molybdenum prealloyed material.

- The materials with the highest apparent hardness values (0.5 w/o nickel, 1.5 w/o molybdenum prealloy) did not exhibit the highest tensile strength values. The highest UTS values were determined for the fast cooled version of the 0.85 w/o molybdenum prealloyed material. It was suggested that retained austenite may be one potential cause for the fall off in strength for the molybdenum/nickel material.

ACKNOWLEDGMENTS

The authors wish to thank Ron Fitzpatrick, Craig Gamble, Steve Kolwicz and Jerry Golin for their assistance in preparing, testing and analyzing the samples. The authors are very grateful to Tom Murphy for his assistance in interpreting the microstructures. We would also like to thank Shirley Tworzydlo for her assistance in the preparation of the manuscript. We would particularly like to thank the staffs at Clarion Sintered Metals, Inc. and Abbott Furnace Company for their invaluable expertise and help in performing the sintering.

REFERENCES

1. Causton, R.J., Fulmer, J.J., “Sinter-Hardening Low-Alloy Steels”, Advances in Powder Metallurgy & Particulate Materials - 1992, Vol.5 , p.17, Metal Powder Industries Federation, Princeton, NJ.

2. Gangnè, M., Trudel, Y., “Effects of Post-Sintering Cooling on the Properties of Low Alloy Sintered Materials”, Advances in Powder Metallurgy - 1991, Vol.4, p.115, Metal Powder Industries Federation, Princeton, NJ.

3. Akpan, E., L' Esperance, G., Roy, L., “Case Histories with Sinter Hardening Low Alloy Steel Powder”, Advances in Powder Metallurgy & Particulate Materials - 1993, Vol.4, p. 289, Metal Powder Industries Federation, Princeton, NJ.

4. Atlas of Isothermal Transformation and Cooling Transformation Diagrams, American Society for Metals, Metals Park, Ohio, 1977, p.18,133.

5. ibid., p. 131, 133.

6. Smith, W.F., Principles of Materials Science & Engineering, 2nd Edition, McGraw-Hill, Inc., 1990, p.491.

7. Rutz, H., Hanejko, F., “High Density Processing of High Performance Ferrous Materials”, Advances in Powder Metallurgy & Particulate Materials - 1994, Vol.5, pp 117-133, Metal Powder Industries Federation, Princeton, NJ.

8. “Standard Test Methods for Metal Powders and Powder Metallurgy Products”, Metal Powder Industries Federation, Princeton, NJ, 1996.

9. “Metals Test Methods and Analytical Procedures”, American Society for Testing and Materials, Vol.03.01,1995, Philadelphia, PA.